Thermal and microcanonical treatments of a pairing Hamiltonian

R. Rossignoli*
Departamento de Física Teórica C-XI, Universidad Autónoma de Madrid, E-28049 Madrid, Spain
(Received 26 February 1996)

The validity of microscopic thermal treatments in comparison with microcanonical results is analyzed for the case of a pairing interaction. The approximate evaluation of microcanonical averages by means of saddle point and moment expansion methods is also examined. Results are shown for a 20-level model, where exact microcanonical averages and level densities are compared with exact thermal results and with those given by the BCS and static path approximations. [S0556-2813(96)03408-5]

PACS number(s): 21.10.Ma, 05.30.−d, 21.60.−n, 24.60.−k

I. INTRODUCTION

The microscopic description of small correlated quantum systems like finite nuclei, at finite excitation energies, constitutes a challenge both for many-body approximation methods and for finite temperature statistical treatments [1]. On the one hand, the small finite size of the system originates large fluctuations and concomitant deviations from the behavior predicted by the standard mean field approximations [2–5]. On the other hand, differences of pure statistical origin may arise between microcanonical and thermal treatments, i.e., between results obtained at fixed excitation energy and at fixed temperature, particularly before the level density becomes sufficiently dense. For instance, in heavy nuclei problems of this type may occur in the quasicontinuum region, approximately located below 10 MeV excitation energy from the yrast line. A particular question here is the quenching of pairing effects with increasing excitation energy, in which deviations from the behavior predicted by the thermal BCS approximation or even by an exact thermal calculation may take place.

The inclusion of fluctuations and correlations beyond the thermal mean field can be treated in a fully microscopic manner by means of the path integral representation of the partition function [6–8]. In particular, the static path approximation (SPA) [9–11] provides a simple microscopic method for including the static fluctuations, which can be quite accurate for evaluating partition functions and thermal averages in finite systems with simple separable attractive interactions like pairing, as will be verified. Full Monte Carlo evaluations of the path integral have also been implemented [7,8]. The second problem concerning the difference between microcanonical and microscopic thermal treatments in correlated systems has so far received less attention, in part due to the difficulty of evaluating microcanonical quantities exactly. Microcanonical level densities in pairing systems have been recently calculated by different methods [12,13], but they were compared with macroscopic Fermi-gas results and not with microscopic thermal treatments.

In this work we first review the calculation, in microscopic statistical treatments, of energy level densities and, in particular, expectation values at fixed excitation energy (rather than temperature), by means of the saddle point approximation. Simple general corrections to the standard thermal average are in this way obtained, which can be applied to any microscopic calculation of the partition function. We also derive these corrections by an energy moment expansion method, formally similar to the Lipkin-Nogami approach for number projection.

We then perform an explicit comparison between exact microcanonical and thermal results for a 20-level monopole pairing model, where the pairing Hamiltonian is diagonalized exactly. As thermal results, we consider those obtained in the exact grand canonical, canonical (fixed particle number N), and fixed number parity (N even or odd) ensembles, and then those obtained with the BCS and static path approximations. We also include an effective BCS approach [14] obtained from the SPA.

The statistical methods employed are discussed in Sec. II. In Sec. III we briefly describe the model and the SPA and BCS approximations. Numerical results are given in Sec. IV and conclusions are drawn in Sec. V.

II. STATISTICAL EVALUATION OF LEVEL DENSITIES AND EXPECTATION VALUES

A. Level densities in grand canonical, canonical, and fixed number parity ensembles

Let us consider first a one-component system described by a Hamiltonian $\hat{H}$ and a particle number operator $\hat{N}$. The energy level density for particle number N is

$$\rho(E,N)\equiv\sum_j \delta_{N_jN}\delta(E_j-E)=\mathrm{Tr}[\hat{P}_N\delta(\hat{H}-E)]$$
$$=\frac{1}{(2\pi i)^2}\int_{\beta_0-i\infty}^{\beta_0+i\infty}d\beta e^{\beta E}\int_{\alpha_0-i\pi}^{\alpha_0+i\pi}d\alpha e^{-\alpha N}Z(\beta,\alpha), \tag{1}$$

where j runs over all many-body eigenstates of the system, with energies E_j, Tr is the grand canonical (GC) trace, $\hat{P}_N\equiv\delta_{\hat{N}N}$ is the particle number projector, and

$$Z(\beta,\alpha)\equiv\mathrm{Tr}\exp(-\beta\hat{H}+\alpha\hat{N}) \tag{2}$$

*Permanent address: Departamento de Física, Universidad Nacional de La Plata, c.c. 67, 1900 La Plata, Argentina.

is the GC partition function. Equation (1) is exact, with β_0 and α_0 arbitrary constants in principle. We have assumed $[\hat{H},\hat{N}]=0$.

The standard procedure to evaluate Eq. (1) in a many-body system is to apply the saddle point approximation, in which the logarithm of the integrand is expanded up to second order in β and α around its stationary point. This leads to the well-known result [15]

$$\rho(E,N)\approx\frac{Z(\beta,\alpha)e^{\beta E-\alpha N}}{[(2\pi)^2\mathrm{Det}(A)]^{1/2}}=\frac{e^{S(\beta,\alpha)}}{[(2\pi)^2\mathrm{Det}(A)]^{1/2}}, \quad (3)$$

where E,N are related with β,α through the equations

$$E=-\frac{\partial}{\partial\beta}\ln Z(\beta,\alpha)=\langle\hat{H}\rangle_{\beta\alpha}, \quad (4)$$

$$N=\frac{\partial}{\partial\alpha}\ln Z(\beta,\alpha)=\langle\hat{N}\rangle_{\beta\alpha}, \quad (5)$$

which determine the maximum of the integrand in Eq. (1) and which define the GC average energy and particle number at temperature $T=1/\beta$ and chemical potential $\mu=\alpha/\beta$, A is the fluctuation matrix

$$A_{ij}=\frac{\partial^2\ln Z(\beta,\alpha)}{\partial\eta_i\partial\eta_j}=\langle\hat{O}_i\hat{O}_j\rangle_{\beta\alpha}-\langle\hat{O}_i\rangle_{\beta\alpha}\langle\hat{O}_j\rangle_{\beta\alpha}, \quad (6)$$

with $\eta=(\beta,\alpha)$, $\hat{O}=(-\hat{H},\hat{N})$, and $S=\ln Z+\beta E-\alpha N$ is the GC entropy. The extension to several components $\hat{N}_i$ is straightforward.

The validity of a thermal GC description is essentially based on the accuracy of the saddle point approximation (3). Except for very low temperatures or excitation energies (i.e., T smaller than the characteristic single-particle level spacing) the approximation (3) leads to a smooth density which is normally very accurate for estimating the mean $\rho(E,N)$ over an energy bin larger than the average level spacing. Nevertheless, in correlated finite systems particular situations at low temperatures may exist where the thermal GC description can be less accurate, even if the *exact* GC partition function is calculated. This may occur, for instance, when an oscillatory or sharp behavior of the average level density, either as a function of N or E, takes place. Moreover, particular phases may become unstable in a GC ensemble as $T\to 0$, as will be here seen for the case of an odd system with a pairing interaction, where a standard GC treatment leads to the wrong $T=0$ limit (see section 3).

When the problems are associated with the variable N, they can be solved by considering a canonical ensemble, in which the particle number is strictly fixed. This amounts to integrate α exactly in Eq. (1). The canonical partition function for a system with N particles is

$$Z_N(\beta)\equiv\mathrm{Tr}[\hat{P}_N\exp(-\beta\hat{H})]=\frac{1}{2\pi i}\int_{\alpha_0-i\pi}^{\alpha_0+i\pi}d\alpha e^{-\alpha N}Z(\beta,\alpha), \quad (7)$$

and the saddle point approximation to the level density, applied now only to the β integral in Eq. (1), leads to

$$\rho(E,N)\approx\frac{Z_N(\beta)e^{\beta E}}{[2\pi\partial^2\ln Z_N/\partial\beta^2]^{1/2}}=\frac{e^{S_N(\beta)}}{[2\pi\partial^2\ln Z_N/\partial\beta^2]^{1/2}}, \quad (8)$$

where E is the canonical average

$$E=-\frac{\partial}{\partial\beta}\ln Z_N(\beta)=\langle\hat{H}\rangle_{\beta N}, \quad (9)$$

and $S_N=\ln Z_N+\beta E$ is the canonical entropy. Except for the particular cases mentioned above, the difference between Eqs. (3) and (8) is normally negligible (see for instance [16]), provided of course that they are compared *at the same* E (and N), rather than at the same temperature. Note that for the same T, the energies (4) and (9) will differ, due to the number fluctuations present in Eq. (4).

In some cases, as in the odd system mentioned above, the wrong $T=0$ limit of the GC ensemble is just caused by the simultaneous presence of states with N even and odd in the partition function. The problems can then be removed by keeping just the even or odd components, without actually needing to employ the canonical ensemble. The fixed number parity partition function is

$$\begin{aligned}Z_\tau(\beta,\alpha)&\equiv\mathrm{Tr}[\hat{P}_\tau\exp(-\beta\hat{H}+\alpha\hat{N})]\\&=\tfrac{1}{2}[Z(\beta,\alpha)+\tau Z(\beta,\alpha+i\pi)],\end{aligned} \quad (10)$$

where $\hat{P}_\tau=\frac{1}{2}(1+\tau e^{i\pi\hat{N}})$ is the number parity projector, which projects states with N even (odd) for $\tau=+1$ (-1). The level density is in this case given by

$$\rho(E,N)\approx\frac{2Z_\tau(\beta,\alpha)e^{\beta E-\alpha N}}{[(2\pi)^2\mathrm{Det}(A)]^{1/2}}=\frac{2e^{S_\tau(\beta,\alpha)}}{[(2\pi)^2\mathrm{Det}(A)]^{1/2}}, \quad (11)$$

with $E=-\partial\ln Z_\tau/\partial\beta$, $N=\partial\ln Z_\tau/\partial\alpha$, $A_{ij}=\partial^2\ln Z_\tau/\partial\eta_i\partial\eta_j$, and where the factor 2 arises from the spacing $\Delta N=2$ [an interval of length π is now sufficient in the α integral in Eq. (1), with a prefactor $2/(2\pi i)^2$]. In approximate many-body treatments, this projection may be easier to apply than the canonical projection. Nevertheless, except for low temperatures in the cases mentioned above, the difference between Eqs. (11) and (3) is negligible.

B. Saddle point approximation for microcanonical expectation values

Let us examine now the evaluation of expectation values at a fixed energy E. The microcanonical average of an operator $\hat{Q}$ is given by

$$\begin{aligned}\langle\hat{Q}\rangle_{EN}&\equiv\mathrm{Tr}[\hat{P}_N\delta(\hat{H}-E)\hat{Q}]/\rho(E,N)\\&=\frac{1}{\rho(E,N)(2\pi i)^2}\int_{\beta_0-i\infty}^{\beta_0+i\infty}d\beta e^{\beta E}\\&\quad\times\int_{\alpha_0-i\pi}^{\alpha_0+i\pi}d\alpha e^{-\alpha N}Z(\beta,\alpha)\langle\hat{Q}\rangle_{\beta\alpha}\end{aligned} \quad (12)$$

where

$$\langle \hat{Q} \rangle_{\beta\alpha} \equiv \mathrm{Tr}[\exp(-\beta\hat{H}+\alpha\hat{N})\hat{Q}]/Z(\beta,\alpha) \tag{13}$$

is the GC average. Whereas $\langle \hat{Q} \rangle_{EN}$ is the average for fixed energy and particle number, $\langle \hat{Q} \rangle_{\beta\alpha}$ is an average for fixed temperature and chemical potential. In the standard thermal approach however, both quantities are simply identified, i.e.,

$$\langle \hat{Q} \rangle_{EN} \approx \langle \hat{Q} \rangle_{\beta\alpha}, \tag{14}$$

where E,N are the GC averages (4) and (5). Nevertheless, $\langle \hat{Q} \rangle_{\beta\alpha}$ contains fluctuations both in E and N. Effects from the determinant in a saddle point approximation of Eq. (12) are missing in Eq. (14), and will now be derived.

It is possible in principle to evaluate the integrals in Eq. (12) directly in the saddle point approximation [17], but we shall employ here a slightly simpler approach. Equations (12) and (13) can be expressed as

$$\langle \hat{Q} \rangle_{EN} = \frac{\partial}{\partial\lambda} \ln\, \rho(E,N,\lambda)|_{\lambda=0}, \tag{15}$$

$$\langle \hat{Q} \rangle_{\beta\alpha} = \frac{\partial}{\partial\lambda} \ln\, Z(\beta,\alpha,\lambda)|_{\lambda=0}, \tag{16}$$

with

$$\rho(E,N,\lambda) = \mathrm{Tr}[\hat{P}_N \delta(\hat{H}-E)\exp(\lambda\hat{Q})] \approx \rho(E,N)(1+\lambda\langle \hat{Q} \rangle_{EN}), \tag{17}$$

$$Z(\beta,\alpha,\lambda) = \mathrm{Tr}\, \exp(-\beta\hat{H}+\alpha\hat{N}+\lambda\hat{Q}) \approx Z(\beta,\alpha)(1+\lambda\langle \hat{Q} \rangle_{\beta\alpha}), \tag{18}$$

where Eqs. (17) and (18) hold up to order λ. Equations (17) and (18) are related by an equation similar to (1) (this would hold to all orders if $[\hat{Q},\hat{H}]=0$, $[\hat{Q},\hat{N}]=0$), so that in the saddle point approximation,

$$\rho(E,N,\lambda) \approx \frac{Z(\beta,\alpha,\lambda)e^{\beta E-\alpha N}}{[(2\pi)^2 \mathrm{Det}(A)]^{1/2}}, \tag{19}$$

where $E=-\partial \ln Z(\beta,\alpha,\lambda)/\partial\beta$, $N=\partial \ln Z(\beta,\alpha,\lambda)/\partial\alpha$, and $A_{ij}=\partial^2 \ln Z(\beta,\alpha,\lambda)/\partial\eta_i\partial\eta_j$, with $\eta=(\beta,\alpha)$. Thus, Eq. (15) yields

$$\langle \hat{Q} \rangle_{EN} \approx \langle \hat{Q} \rangle_{\beta\alpha} - \tfrac{1}{2}\frac{d}{d\lambda} \ln\, \mathrm{Det}(A)|_{\lambda=0}, \tag{20}$$

where $d/d\lambda$ denotes the derivative at constant E and N, i.e., $d/d\lambda = \partial/\partial\lambda + \Sigma_i (d\eta_i/d\lambda)\partial/\partial\eta_i$, with $d\eta_i/d\lambda = -\Sigma_j A^{-1}_{ij}\partial^2 \ln Z(\beta,\alpha,\lambda)/\partial\lambda\partial\eta_j$, and E,N are again determined by Eqs. (4) and (5). The extension to several components is straightforward.

In a canonical ensemble, Eq. (20) reduces to (we omit for simplicity the subscript N in the following averages)

$$\langle \hat{Q} \rangle_E \approx \langle \hat{Q} \rangle_\beta - \tfrac{1}{2}\frac{[\partial^3/\partial\beta^2\partial\lambda + (d\beta/d\lambda)\partial^3/\partial\beta^3]\ln Z_N(\beta,\lambda)}{(\partial^2/\partial\beta^2)\ln Z_N(\beta,\lambda)}\Big|_{\lambda=0} = \langle \hat{Q} \rangle_\beta - \frac{\langle \hat{Q}'\hat{H}'^2\rangle_\beta \langle \hat{H}'^2\rangle_\beta - \langle \hat{Q}'\hat{H}'\rangle_\beta \langle \hat{H}'^3\rangle_\beta}{2\langle \hat{H}'^2\rangle_\beta^2}, \tag{21}$$

where $E=\langle \hat{H} \rangle_\beta$ is the canonical energy (9),

$$\langle \hat{Q} \rangle_\beta \equiv \mathrm{Tr}[\hat{P}_N \exp(-\beta\hat{H})\hat{Q}]/Z_N(\beta) \tag{22}$$

is the canonical average, $\hat{H}' \equiv \hat{H} - \langle \hat{H} \rangle_\beta$, $\hat{Q}' \equiv \hat{Q} - \langle \hat{Q} \rangle_\beta$ and $d\beta/d\lambda = -\langle \hat{H}'\hat{Q}' \rangle_\beta / \langle \hat{H}'^2 \rangle_\beta$.

The second term on the right-hand side of Eq. (20) or (21) provides a correction to the direct GC or canonical average, which is normally small but nevertheless observable in finite systems (note that it vanishes for $\hat{Q}=\hat{H}$ or $\hat{N}$). The thermal averages (13) or (22), being essentially a Laplace transform, will always be *smoother*, as a function of E, than the microcanonical average, even after averaging $\langle \hat{Q} \rangle_{EN}$ over a sufficiently large energy bin. The expressions (20) and (21) yield instead the correct mean of $\langle \hat{Q} \rangle_{EN}$, although we remark that oscillations or abrupt changes around the value given by Eq. (20) or (21) may still occur in the actual $\langle \hat{Q} \rangle_{EN}$. Results obtained with a direct application of the saddle point method to Eq. (12) [17] (together with a suitable displacement $\hat{Q} \to \hat{Q} + Q_0$ when $\langle \hat{Q} \rangle_{EN}$ exhibits sign changes) are practically equal to those obtained with Eq. (20). This procedure becomes obviously equivalent to Eq. (20) when applied to the operator $\hat{Q}' = (\lambda\hat{Q}+1)$ in the limit $\lambda \to 0$.

A different simple approach for evaluating $\langle \hat{Q} \rangle_{EN}$, based on an energy moment expansion (similar to the Lipkin-Nogami method [18] for number projection), is derived in the Appendix. The ensuing expression involves, however, higher moments of $\hat{H}'$ and is more difficult to apply in the GC ensemble, but results are practically coincident with Eq. (21) in the present statistical situation.

III. APPLICATION TO A PAIRING HAMILTONIAN

A. Hamiltonian and model

We shall consider a monopole pairing interaction restricted to an interval I around the Fermi energy. The Hamiltonian reads

$$\hat{H} = \hat{H}_0 - \tfrac{1}{2}G(\hat{P}^\dagger\hat{P} + \hat{P}\hat{P}^\dagger) \tag{23}$$

$$= \hat{H}_0 - G\hat{P}^\dagger\hat{P} + \tfrac{1}{2}G(\hat{N}_I - \Omega_I), \tag{24}$$

where

$$\hat{H}_0 = \sum_k \varepsilon_k (c_k^\dagger c_k + c_{\bar{k}}^\dagger c_{\bar{k}}) \tag{25}$$

is a single-particle Hamiltonian with time reversal symmetry and

$$\hat{P}^\dagger=\sum_{k\in I} c_k^\dagger c_{\bar{k}}^\dagger, \quad \hat{P}=\sum_{k\in I} c_{\bar{k}} c_k,$$

$$\hat{N}_I=\sum_{k\in I} c_k^\dagger c_k + c_{\bar{k}}^\dagger c_{\bar{k}}, \tag{26}$$

are, respectively, the pairing and number operators in the pairing interval, of total dimension $2\Omega_I$. We have used in Eq. (23) the symmetric form of the pairing interaction, which does not change the chemical potential in the half-filled case with equally spaced single-particle levels. The effect of the term $G(\hat{N}_I-\Omega_I)/2$ is nevertheless irrelevant in the following results.

For a complete exact diagonalization, including all levels as required by a statistical treatment, we have chosen a total of $\Omega=20$ single-particle levels (each with degeneracy 2 due to time reversal symmetry, so that the total number of levels is $2\Omega=40$) with the pairing force acting in the central 10 levels ($\Omega_I=10$). In this case, for the half-filled case ($N=\Omega$), there are a total of $\binom{40}{20}=1.378\times 10^{11}$ many-body states in the canonical ensemble. The many-body states in the pairing interval can be classified according to the number n_2 and n_0 of levels with occupation 2 and 0, with $0\leqslant n_2+n_0\leqslant\Omega_I$ and $N_I=\Omega_I+n_2-n_0$. There are a total of $\binom{\Omega_I}{n_2+n_0}$ different ''multiplets'' of this type, each of dimension $\binom{n_2+n_0}{n_2}$ (which is the dimension of the pairing Hamiltonian matrix in the multiplet) and degeneracy $2^{\Omega_I-n_2-n_0}$ (due to the remaining levels with occupation 1), such that

$$\sum_{n_2,n_0}\delta_{N_I,\Omega_I+n_2-n_0}\binom{\Omega_I}{n_2+n_0}\binom{n_2+n_0}{n_2}2^{\Omega_I-n_2-n_0}=\binom{2\Omega_I}{N_I}.$$

The exact eigenvalues can be calculated by diagonalization of $\hat{H}$ in each multiplet. Exact microcanonical and canonical results for N particles can then be obtained by convolution of results with N_I particles in the interval I and $N-N_I$ particles in the remaining levels.

B. Static path approximation

Let us consider now thermal microscopic many-body approximations. The SPA [9–11,19–22] considers just the static paths in the path integral representation of the partition function obtained with the Hubbard-Stratonovich transformation [6]. These static paths represent the statistical fluctuations around the mean field and are very important in the case of a finite system. In fact, for a pairing Hamiltonian the SPA contains, as we shall see, most of the relevant corrections to the mean field approximation except for low temperatures, at least for quantities like level densities or collective expectation values, becoming exact for high T (in the general case, up to order β in the partition function).

We define first the quasiparticle Hamiltonian

$$\hat{H}(\Delta)\equiv\hat{H}_0-\Delta(\hat{P}^\dagger+\hat{P})+\Delta^2/G, \tag{27}$$

where $\hat{H}_0$ is the Hamiltonian (25). The GC SPA partition function for the Hamiltonian (24) is given by [19]

$$Z_{\rm SPA}(\beta,\alpha)=\frac{2}{GT}\int_0^\infty Z(\beta,\alpha,\Delta)\Delta d\Delta, \tag{28}$$

where

$$Z(\beta,\alpha,\Delta)=\mathrm{Tr}\,\exp[-\beta\hat{H}(\Delta)+\alpha\hat{N}]$$

$$=e^{-\beta(\Delta^2/G+\Sigma_k\varepsilon_k-\mu)}\prod_k 4\cosh^2\frac{\beta E_k}{2}, \tag{29}$$

with E_k the quasiparticle energies

$$E_k=[(\varepsilon_k-\mu)^2+\Delta^2]^{1/2}, \quad k\in I,$$

$$E_k=|\varepsilon_k-\mu| \quad \text{otherwise}. \tag{30}$$

The GC SPA expectation values are

$$\langle\hat{Q}\rangle_{\rm SPA}=\frac{\int_0^\infty Z(\beta,\alpha,\Delta)\langle\hat{Q}\rangle_\Delta\Delta d\Delta}{\int_0^\infty Z(\beta,\alpha,\Delta)\Delta d\Delta}, \tag{31}$$

with

$$\langle\hat{Q}\rangle_\Delta\equiv\mathrm{Tr}\{\exp[-\beta\hat{H}(\Delta)+\alpha\hat{N}]\hat{Q}\}/Z(\beta,\alpha,\Delta), \tag{32}$$

the independent quasiparticle averages. In particular,

$$\langle\hat{P}^\dagger\hat{P}\rangle_\Delta=\langle\hat{P}^\dagger\rangle_\Delta\langle\hat{P}\rangle_\Delta+\sum_{k\in I}\langle c_k^\dagger c_k\rangle_\Delta\langle c_{\bar{k}}^\dagger c_{\bar{k}}\rangle_\Delta, \tag{33}$$

$$\langle\hat{P}\rangle_\Delta=\tfrac{1}{2}\Delta\sum_{k\in I}E_k^{-1}\tanh\frac{\beta E_k}{2}, \tag{34}$$

$$\langle c_k^\dagger c_k\rangle_\Delta=\langle c_{\bar{k}}^\dagger c_{\bar{k}}\rangle_\Delta=\tfrac{1}{2}\left(1-\frac{\varepsilon_k-\mu}{E_k}\tanh\frac{\beta E_k}{2}\right). \tag{35}$$

The second term on the right-hand side of Eq. (33) is the exchange contribution.

The energy derived from Eq. (28) can be expressed as [14]

$$E_{\rm SPA}\equiv-\frac{\partial}{\partial\beta}\ln Z_{\rm SPA}=\langle\hat{H}_0\rangle_{\rm SPA}-\tfrac{1}{2}\langle\Delta(\hat{P}^\dagger+\hat{P})\rangle_{\rm SPA}$$

$$=\langle\hat{H}_0\rangle_{\rm SPA}-G^{-1}\langle\Delta^2\rangle_{\rm SPA}+T. \tag{36}$$

This energy becomes exact for high T but as $T\to 0$, it approaches the BCS energy, without exchange terms. The energy expectation value

$$\langle\hat{H}\rangle_{\rm SPA}\equiv\langle\hat{H}_0\rangle_{\rm SPA}-\tfrac{1}{2}G\langle\hat{P}^\dagger\hat{P}+\hat{P}\hat{P}^\dagger\rangle_{\rm SPA} \tag{37}$$

$$=E_{\rm SPA}-\tfrac{1}{2}G\langle\hat{P}'^\dagger\hat{P}'+\hat{P}'\hat{P}'^\dagger\rangle_{\rm SPA}+T, \tag{38}$$

where $\hat{P}'=\hat{P}-\Delta/G$, contains the exchange terms and hence differs from Eq. (36) for low T, although for $T\to\infty$ and μ finite, both Eqs. (36) and (37) become exact and their difference vanishes.

The SPA can in principle also be applied in a canonical ensemble. In this case, since $[\hat{H}(\Delta),\hat{N}]\neq 0$, the exact finite temperature number projection [23–25] introduces, in addi-

tion to the statistical corrections, quantum correlations which improve the $T=0$ limit of expectation values (since the projected BCS vacuum is approached as $T\to 0$). These quantum corrections are, however, less important for larger temperatures. Number parity projection is straightforward to implement since $e^{i\pi\hat{N}}=e^{i\pi\hat{N}_q}$, where $\hat{N}_q$ is the quasiparticle number operator ($[\hat{N}_q(\Delta),\hat{H}(\Delta)]=0$), but is only relevant at low temperatures for an odd system. The microcanonical corrections of Eq. (20) can in principle also be implemented, although in the low T region they may be in fact of the same order as the correlations omitted in the SPA.

C. BCS and effective BCS approximations

The standard BCS approximation, without exchange terms, is based on an independent quasiparticle Hamiltonian of the form (27). The BCS partition function is

$$Z_{\rm BCS}=Z(\beta,\alpha,\Delta_0), \tag{39}$$

where Δ_0 is obtained from the well-known gap equation

$$\Delta_0-G\langle\hat{P}\rangle_{\Delta_0}=0, \tag{40}$$

which determines the maximum of $Z(\beta,\alpha,\Delta)$. This equation leads to the superfluid to normal transition at the critical temperature determined by $(G/2)\Sigma_{k\epsilon I}E_k^{-1}\tanh(\beta_c E_k/2)=1$, such that $\Delta_0=0$ for $T>T_c$. Hence, using Eq. (33) and (40),

$$\langle\hat{P}^\dagger\hat{P}\rangle_{\rm BCS}\equiv\langle\hat{P}^\dagger\hat{P}\rangle_{\Delta_0}=\Delta_0^2/G^2+\sum_{k\in I}\langle c_k^\dagger c_k\rangle_{\Delta_0}\langle c_{\bar{k}}^\dagger c_{\bar{k}}\rangle_{\Delta_0},$$

reduces, for $T>T_c$, to the exchange contribution. The transition appears, however, washed out in a finite system, both in the SPA or in an exact thermal treatment.

The inclusion of the exchange term in the variation of the BCS free energy $\langle\hat{H}\rangle_\Delta-TS$ leads to the replacement of ε_k by ε_k' for $k\in I$ in Eqs. (29) and (30), with ε_k' determined by the additional self-consistent equations $\varepsilon_k'=\varepsilon_k-G(\langle c_k^\dagger c_k\rangle_{\Delta_0}-1/2)$. This does not change, however, the sharp character of the transition, and affects only slightly the value of T_c. It is important nevertheless to consider the exchange term, at least after variation, when a comparison with exact thermal averages is performed.

A straightforward improved effective BCS approximation can be obtained if the measure Δ is taken into account when the maximum of the integrand in Eq. (28) is determined [14]. This leads to an effective value Δ_0' determined by the equation

$$\Delta_0'-G\langle\hat{P}\rangle_{\Delta_0'}-\tfrac{1}{2}GT/\Delta_0'=0, \tag{41}$$

whose solution for finite G is *smooth* as a function of T and does not vanish for $T>0$, so that the sharp superconducting to normal transition is washed out in a finite system. This behavior reflects that obtained in a thermal BCS treatment with rigorous number projection [24] or symmetry restoration [14,26] before variation, in which the sharp pairing transition is also smoothed out.

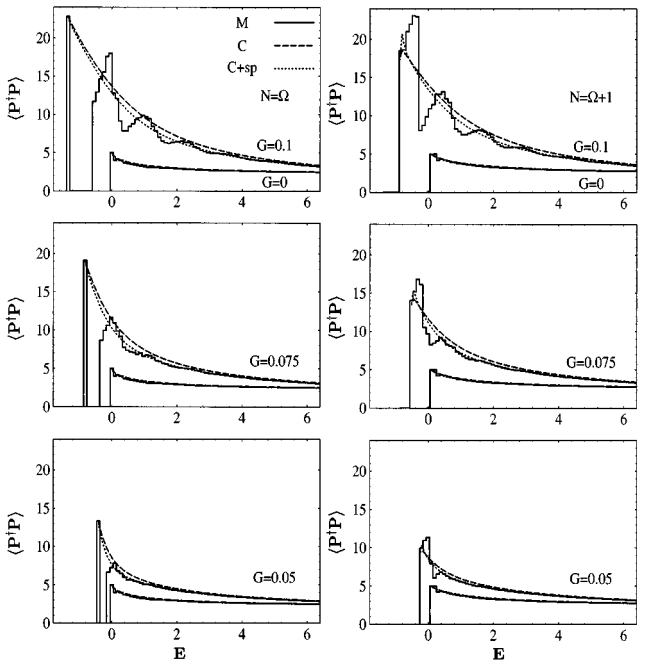

FIG. 1. Exact microcanonical (M) and canonical (C) averages of the pairing correlation operator $\hat{P}^\dagger\hat{P}$, as a function of energy in the $\Omega=20$ level model, for different pairing strengths G in the even (left) and odd (right) systems. C denotes the thermal canonical average (22), $C+$sp the full saddle point expression (21). The result for $G=0$ is shown for reference in all cases, and the energy is measured from the ground state of the even $G=0$ system. The single-particle level spacing of the model, fixing the energy units, is 0.1.

The solution of Eq. (41) can be employed for an evaluation of the SPA integral (28) in the saddle point approximation [14], which yields

$$Z_{\rm SPA}\approx\sqrt{\frac{4\pi}{GT}}\Delta_0' D^{-1/2}Z(\beta,\alpha,\Delta_0') \tag{42}$$

with $D=(GT/2)\left|\partial^2\ln[\Delta Z(\beta,\alpha,\Delta)]/\partial\Delta^2\right|$ a dimensionless factor, roughly of order 1. In spite of its simplicity, Eq. (42) is quite accurate for evaluating the SPA level density and allows for a rapid identification of the most prominent SPA corrections to the standard BCS, namely, the smooth behavior and the enhancement factor $\Delta_0'\sqrt{4\pi/GT}$ in comparison with the BCS partition function (39). Note that owing to the transition at $T=T_c$, the saddle point approximation to Eq. (28) around the ordinary BCS solution is not accurate in the whole transitional region.

IV. RESULTS

A. Exact thermal and microcanonical results

We consider first a uniform single-particle spectrum, with spacing ε ($\varepsilon\equiv\varepsilon_{k+1}-\varepsilon_k$). For $N=\Omega=20$, a superfluid ground state occurs in this case for $G/\varepsilon>0.18$. In the figures we have set $\varepsilon=0.1$ (arbitrary units) and the exact microcanonical quantities plotted correspond to an energy bin $\Delta E=\varepsilon$.

Figure 1 depicts the exact microcanonical expectation

value of $\hat{P}^\dagger\hat{P}$ for various values of G, together with the exact canonical thermal result [obtained using the exact eigenvalues and eigenvectors in (22)]. We note that $\langle\hat{P}^\dagger\hat{P}\rangle_E$ is the total strength of the average two-particle pair transfer function at energy E,

$$\langle\hat{P}^\dagger\hat{P}\rangle_E=\int dE'S(E,E'),$$

$$S(E,E')=\frac{\Sigma_{j,k}|\langle k|\hat{P}|j\rangle|^2\delta(E'-E_k+E_j)\delta(E-E_j)}{\Sigma_j\delta(E-E_j)}.$$

It is first seen that oscillations in the microcanonical expectation value at low excitation energies, both for the even and odd systems, develop as the strength G increases, which are not reproduced by the thermal treatments. These oscillations reflect those arising in the degenerate limit, approached as $G\rightarrow\infty$, in which the energy eigenvalues, the pairing expectation value and the corresponding degeneracies, considering only the pairing interval and setting $\varepsilon_k=0$, are given by [27]

$$E_{QM}=-G[Q(Q+1)-M^2], \tag{43}$$

$$\langle\hat{P}^\dagger\hat{P}\rangle_{QM}=Q(Q+1)-M^2+M, \tag{44}$$

$$D(Q)=\binom{2\Omega_I}{\Omega_I-2Q}-\binom{2\Omega_I}{\Omega_I-2Q-2}, \tag{45}$$

where $M=(N_I-\Omega_I)/2$ and Q is the quasispin, with $|M|\leqslant Q\leqslant\Omega_I/2$ (Q is half integer for N_I odd). The seniority is Ω_I-2Q, and the superfluid ground state corresponds to $Q=\Omega_I/2$.

This limit leads, for large but finite G, to a series of smoothed peaks in $\langle\hat{P}^\dagger\hat{P}\rangle_E$, centered at the energies (43), with a characteristic energy spacing $\Delta_E=E_{QM}-E_{Q-1,M}=2GQ$, i.e., $\Delta_E\approx G\Omega_I$ for the first peaks. The peaks become washed out as the excitation energy increases. As G decreases, only the first peak remains noticeable, which corresponds in the even system to the superfluid ground state and in the odd system to the ground state ''band'' with a single unpaired particle [$Q=(\Omega_I-1)/2$]. The peaks in the odd system are obviously located at the minima of the even system.

Nevertheless, as the excitation energy increases, the thermal canonical treatment becomes very accurate, particularly when the full saddle point expression (21) is employed. The direct average $\langle\hat{P}^\dagger\hat{P}\rangle_\beta$ lies slightly above $\langle\hat{P}^\dagger\hat{P}\rangle_E$, but the corrected expression (21) accurately follows the mean of the microcanonical average. Results obtained with the moment expansion method up to second order, Eq. (A6), are undistinguishable from those given by Eq. (21). Higher order expansions [$L>2$ in Eq. (A1)] do not lead to a correct reproduction of the microcanonical oscillations either, and require a high accuracy in the determination of moments $\langle\hat{H}'^n\rangle_\beta$ with large n (i.e., $n\leqslant 8$ for $L=4$).

Another feature to be observed is that above the low energy region, the quenching of $\langle\hat{P}^\dagger\hat{P}\rangle_E$ as E increases is smooth, without sharp transitions, with a nonvanishing enhancement over the value obtained for zero strength. Note

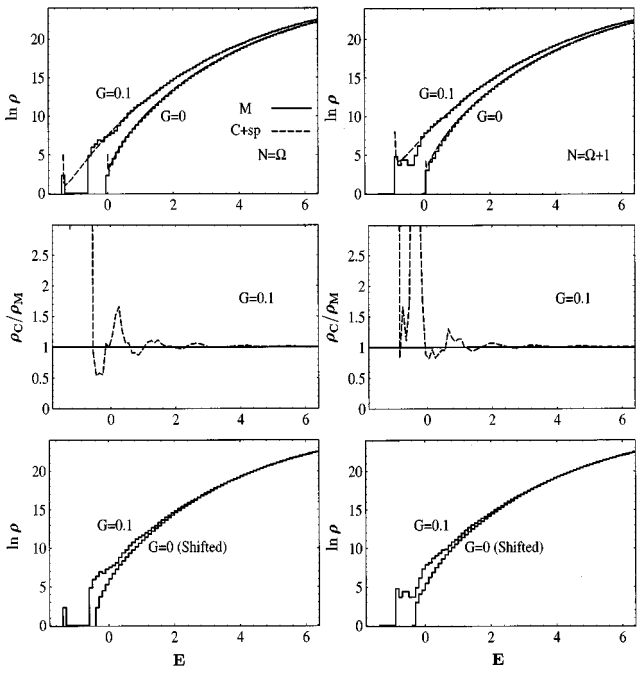

FIG. 2. Top: Logarithm of the energy level density in the even (left) and odd (right) systems, for $G=0$ and 0.1. M denotes the exact microcanonical result, C+sp the canonical saddle point expression (8). Center: Quotient between the canonical and microcanonical level densities for $G=0.1$ (dashed line). Bottom: Comparison between the $G=0.1$ and the shifted $G=0$ level densities. The energy shift is such that both curves practically overlap for high E.

that the BCS superfluid to normal transitions take place at $E\approx$ 1.2, 0.2, and 0 for $G=$ 0.1, 0.075, and 0.05, respectively (see Fig. 5).

The oscillations are less noticeable in the level density (Fig. 2). Except for very low E (i.e., in the gap region) the saddle point expression (8) is very accurate, even for $G=0.1$, and the oscillations of the microcanonical density around this value decrease very rapidly with excitation energy. The error between both is less than 15% for $E>1$ and less than 5% for $E>3$. In comparison with the level density for $G=0$, an enhancement at a fixed energy E in an absolute scale occurs in the level density for $G>0$, which reflects the shift towards lower energies of the spectrum. However, both densities can be made practically coincident at high E if the $G=0$ density is shifted by a suitable amount, as seen in the bottom panel. This entails a very weak dependence of the appropriately displaced densities on the strength for high E. Nevertheless, with this shift an enhancement over the $G=0$ value subsists for low energies.

The previous figures depict only exact canonical (fixed particle number) thermal results. A comparison between the exact canonical and GC results is made in Fig. 3. For the even system, the differences between canonical and GC direct averages at a fixed temperature are small, but can nevertheless be noticed, especially in the energy. However, for the quantities obtained in the saddle point approximation, like the level densities (3) and (8), and the corrected expressions (20) and (21), canonical and GC results are practically coincident when plotted as a function of the corresponding

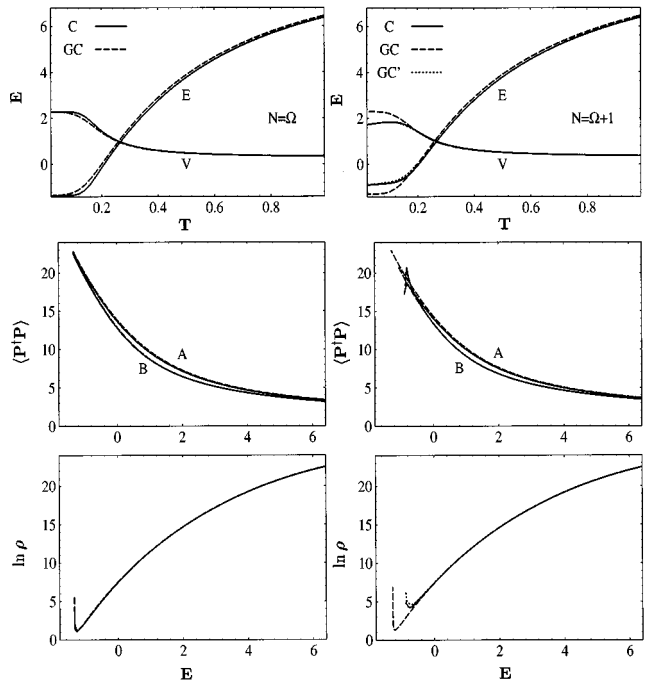

FIG. 3. Exact grand canonical (GC) and canonical (C) thermal results for $G=0.1$ in the even (left) and odd (right) systems. GC′ (right) denotes the number parity projected ensemble. Top: Average energy E and pairing energy $V\equiv G\langle\hat{P}^\dagger\hat{P}\rangle$ as a function of temperature. Center and bottom: Canonical and GC results (practically overlapping) for $\langle\hat{P}^\dagger\hat{P}\rangle$ and the level density [Eqs. (8) and (3)], as a function of the corresponding energy. At center, A depicts the direct averages (22) (C) and (13) (GC), B the saddle point results (21) (C) and (20) (GC).

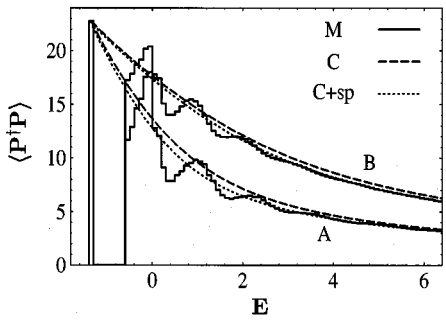

FIG. 4. Comparison between exact microcanonical and canonical results for a one-component system (A) and a noninteracting two component system (B). The same parameters of Fig. 1 are used in both components, with $G=0.1$, and the ground state energy in B is set equal to that of A. $C+$sp depicts the saddle point result (21).

excitation energy (rather than temperature). The same holds for the odd system, except that in this case the exact GC treatment leads to the wrong $T=0$ limit due to the lack of blocking effects, approaching as $T\to 0$ a mixture of the ground states of the $N_I=\Omega$ and $N_I=\Omega+2$ systems rather than the ground state of the odd system (whose energy lies above that of the neighbor even systems). This low T effect is corrected in the number parity projected treatment (and obviously also in the canonical treatment) which for higher values of E and T, practically coincides with the standard GC treatment.

In a noninteracting two-component system, the microcanonical deviations from the thermal treatments become smaller when plotted as a function of the total energy, as fluctuations in the energy of a particular component now occur. In a nucleus, the present situation would approximately apply when valence protons and neutrons occupy different major shells, as in heavy nuclei, in which case one can neglect the pairing interaction between them. Let us consider for instance a two-component system with exactly the same Hamiltonians and strengths, without interaction between them. At a fixed temperature T, the total excitation energy is now $E=E_1+E_2=2E_1$, whereas the thermal average $\langle\hat{P}_i^\dagger\hat{P}_i\rangle_\beta$ ($i=1,2$) remains unaltered, both in the canonical and GC ensembles. Hence, when plotted in terms of the total energy, the effect in the thermal average is just the scaling $E\to 2E$. The correction term in Eqs. (20) and (21) is however reduced by half, which indicates a smaller mean deviation between the microcanonical and thermal average. Figure 4 depicts $\langle\hat{P}_i^\dagger\hat{P}_i\rangle_E$ ($i=1$ or 2) in this situation. The above scaling is verified for large E in the microcanonical average, but the oscillations around the thermal average, though smaller, subsist and do not follow the above scaling. For example, in the present case the first excited state of the combined system has the same excitation energy as that of the single system, but is degenerate, with one of the two components in the first excited state and the other in the ground state. Hence, at this energy $\langle\hat{P}_i^\dagger\hat{P}_i\rangle_E$ will be the average of the values in both states, which leads to a smoothing effect without scaling.

B. Comparison with the static path and BCS approximations

Let us examine now the validity of the microscopic many-body approximations. Figure 5 depicts, for the even system, BCS, SPA, and effective BCS results, plotted in terms of the corresponding energy, together with the exact microcanonical or GC results. The BCS average of $\langle\hat{P}^\dagger\hat{P}\rangle$ compares rather bad with the exact value. For $T>T_c$, it coincides with the value for $G=0$ (i.e., the exchange contribution) whereas for $T<T_c$ its decrease is practically linear, with a slope discontinuity at $T=T_c$. On the other hand, it is remarkable that the SPA average $\langle\hat{P}^\dagger\hat{P}\rangle_{\rm SPA}$ practically coincides with the exact thermal result when plotted in terms of the SPA excitation energy [which is here calculated according to Eq. (37)]. The simple effective BCS estimation $\langle\hat{P}^\dagger\hat{P}\rangle_{\Delta_0'}$, obtained with the solution of eq. (41), gives also a straightforward improvement over the standard BCS value. Inclusion of the microcanonical corrections (20) in the SPA would lead to results practically coincident with those of the exact GC+sp treatment, except for low energies.

The pairing energy is quadratic in the gap. In order to visualize more clearly the deviation from the $G=0$ value at high E, we have also plotted in Fig. 5 the effective density gap, defined as

$$\Delta_{\rm eff}\equiv G[\langle\hat{P}^\dagger\hat{P}\rangle_{T,G}-\langle\hat{P}^\dagger\hat{P}\rangle_{T,G=0}]^{1/2}. \tag{46}$$

In BCS, the value of $\Delta_{\rm eff}$ vanishes for $T>T_c$, whereas for $T<T_c$ practically coincides with the normal gap Δ_0, as the

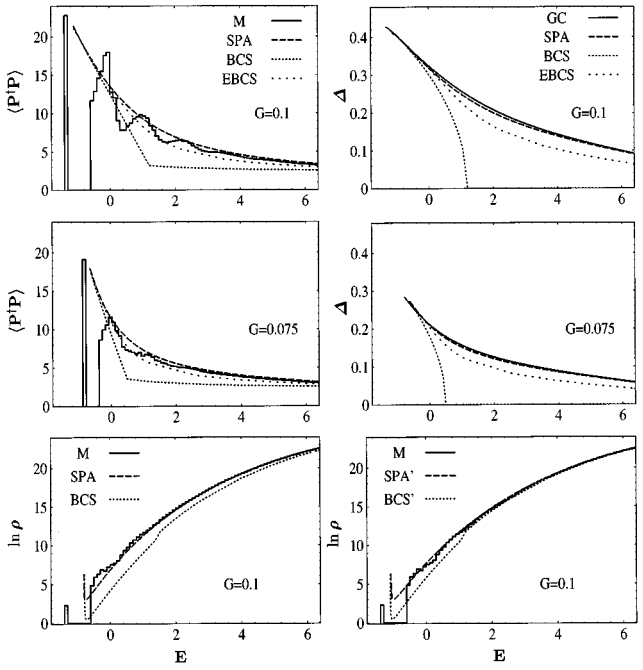

FIG. 5. Comparison with thermal GC many-body approximations. Top and center: The exact microcanonical (M) average of $\hat{P}^\dagger\hat{P}$ (left) and the exact GC value of the effective gap (46) (right) are compared with the results obtained in the static path (SPA), BCS and effective BCS (EBCS) approximations. Bottom: Exact and approximate level densities. SPA and BCS results correspond to the saddle point equation (3). At right, SPA′ and BCS′ indicate results with the inclusion of the exchange term in the energy (see text).

exchange term varies only weakly with G. In the SPA, $\Delta_{\rm eff}$ is practically equal to the direct average $G\langle\langle\hat{P}^\dagger\rangle_\Delta\langle\hat{P}\rangle_\Delta\rangle^{1/2}_{\rm SPA}$ obtained by neglecting the exchange term in Eq. (33). Hence, Eq. (46) can be taken as a measure of the collective content in the pairing energy. The agreement between the exact GC thermal result and the SPA value for $\Delta_{\rm eff}$ is clearly seen. In contrast with BCS, a rather large value of $\Delta_{\rm eff}$ subsists for $T>T_c$. For $T\to\infty$, the SPA yields in the present finite space the limit

$$\Delta_{\rm eff}\to\frac{1}{4}\Omega_I G\sqrt{G/T}=\frac{1}{4}g\sqrt{g/\Omega_I T}, \tag{47}$$

with $g=\Omega_I G$, so that $\Delta_{\rm eff}\propto(\Omega_I T)^{-1/2}$ for high T.

For the level density, the BCS result calculated with Eqs. (3) and (39) exhibits a discontinuity at $T=T_c$ and lies below the exact level density even beyond the transition. The BCS result improves when the exchange term is included (bottom right figure), which amounts practically to a shift in the energy since it is almost constant with T. In this case the result is correct beyond the transition, where the BCS density is essentially that for $G=0$ with an energy shift given by the exchange term. This is therefore in agreement with the coincidence with the shifted $G=0$ density for high E (Fig. 2). Nevertheless, a low value subsists for $T<T_c$, which, as discussed in [14,26], is associated with the small value of the BCS entropy in the superfluid phase, due to the breaking of number conservation and the ensuing U(1) gauge symmetry.

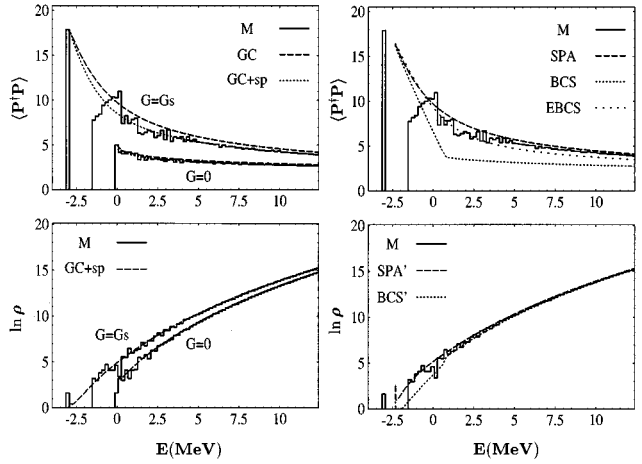

FIG. 6. Results for a nonuniform single-particle level spacing and a scaled strength G_s (see text). The exact microcanonical results for $\langle\hat{P}^\dagger\hat{P}\rangle$ and the level density (in MeV^{-1}) are compared with the exact GC results (left) and with SPA and BCS results (right). Exact results for $G=0$ are also depicted (left).

The SPA result, obtained with Eqs. (3) and (28), is clearly exact for high T but slightly underestimates the exact result for low T, essentially due to the omission of the exchange term in the energy (36). The SPA results in this region improve if plotted just in terms of the full energy (37) (lower figure), which contains the exchange term, although a more consistent improvement can be done with the SPA+RPA treatment [28,29]. Level density results obtained with saddle point approximation (42) to the SPA partition function, calculated around the effective BCS solution, practically overlap with the full SPA results [14]. The enhancement factor present in (42) corrects the low BCS entropy and level density in the superfluid phase.

Finally, we depict in Fig. 6 results for a nonuniform single-particle spectrum, which should be closer to a realistic situation. We have chosen the central 20 neutron single-particle energies around the Fermi level in ^{164}Er, obtained with a deformed quadrupole single particle Hamiltonian $\hat{H}_0-\beta\hat{Q}_0$ within the Baranger-Kumar configuration space [30]. We employed a scaled pairing strength $G_s=44/164$ MeV, which reproduces approximately the same gap as in the full configuration space. The energy bin of the microcanonical calculation is 0.2 MeV. There are now more irregularities present in the exact microcanonical results (small fluctuations around the thermal values appear now even for $G=0$, as seen in the level density) but they are otherwise similar to the previous ones, particularly to the case $G=0.075$ (larger oscillations would occur for a higher strength G_s). Thermal GC results obtained with the expressions (20) and (3) yield again the correct mean of the microcanonical averages. Note however that the difference between the direct average (13) and the saddle point expression (20) is observable. SPA results are again in good agreement with the exact GC thermal values, and significant differences with the BCS results subsist.

V. CONCLUSIONS

The validity of microscopic thermal descriptions in comparison with exact microcanonical results has been analyzed.

The present considerations apply to any microscopic thermal calculation. It is first seen that by proper use of the saddle point method in thermal treatments, simple general expressions for level densities and also expectation values at fixed excitation energy can be obtained, which yield the correct mean of the exact microcanonical average and which are very accurate for high excitation energies if the partition function is correctly calculated. Nevertheless, at small excitation energies fluctuations and oscillations around the thermal or saddle point values may occur in microcanonical quantities, which can be particularly noticeable in correlated systems and in certain observables, as we have seen in the case of pairing. The statistical calculation of these effects would thus require a more refined evaluation of the inverse β integrals in Eqs. (1) and (12). Simple moment expansion methods yield results which are qualitatively similar at finite temperature to those of the saddle point method. Maximum entropy reconstruction techniques, like those employed for recovering the strength function from the response function [8], or pseudoinverse methods [31], might provide, for instance, an improved numerical evaluation of the inverse transforms.

The obvious advantage of thermal treatments is, however, that the partition function in finite correlated many-body systems can in principle be quite accurately calculated, using for instance Monte Carlo path integral methods [8]. For the pairing Hamiltonian considered, even a simple treatment like the SPA yields results which are remarkably accurate in a statistical context, although for more realistic interactions the SPA can be less adequate, particularly at low temperatures [7,8]. Nevertheless, the present results indicate that the inclusion of additional correlations at low temperatures should be complemented in principle with the inclusion of microcanonical corrections. On the other hand, standard thermal methods like the mean field approximation (BCS in the present case) are confirmed to exhibit significant deviations from the exact results. At least, an improved saddle point evaluation of the SPA, like the effective BCS approach discussed here, should be considered.

ACKNOWLEDGMENTS

Stimulating discussions with J. L. Egido are gratefully acknowledged. This work was supported by DGICyT, Spain, under a grant for Estancias Temporales de Científicos y Tecnólogos Extranjeros. R.R. is supported by CICPBA, of Argentina and acknowledges a grant from Fundación Antorchas.

APPENDIX: MOMENT EXPANSION METHOD FOR MICROCANONICAL AVERAGES

Let us consider first a canonical ensemble, and assume an expansion of the microcanonical average of the form

$$\langle \hat{Q} \rangle_E = \sum_{i=0}^{L} \lambda_i (E - E_0)^i, \tag{A1}$$

which becomes in principle exact for sufficiently large L for a finite discrete spectrum. For a finite L, the unknown parameters λ_i can be obtained from the averages

$$M_i(\beta) \equiv \langle \hat{Q} (\hat{H} - E_0)^i \rangle_\beta = \sum_{j=0}^{L} \lambda_j \langle (\hat{H} - E_0)^{i+j} \rangle_\beta,$$

$$i = 0, \ldots, L, \tag{A2}$$

which can be rewritten in matrix notation as

$$\boldsymbol{M}(\beta) = G(\beta) \boldsymbol{\lambda}, \quad G_{ij}(\beta) = \langle (\hat{H} - E_0)^{i+j} \rangle_\beta. \tag{A3}$$

The parameters λ_i will then be given by

$$\boldsymbol{\lambda} = G^{-1}(\beta) \boldsymbol{M}(\beta), \tag{A4}$$

and will in general depend on temperature for finite L. Equation (A1) is then to be employed at the corresponding average energy $E = \langle \hat{H} \rangle_\beta$. The expansion (A1) is exact for $\hat{Q} = \Sigma_{i=0}^{L} q_i (\hat{H} - E_0)^i$, i.e., a polynomial of degree L in $\hat{H}$, in which case Eq. (A4) yields $\lambda_i = q_i$, independent of temperature.

In the above expressions, E_0 is arbitrary. Setting now $E_0 = \langle \hat{H} \rangle_\beta$, Eq. (A1) leads, for $E = \langle \hat{H} \rangle_\beta$, to

$$\langle \hat{Q} \rangle_E = \lambda_0(\beta) = \langle \hat{Q} \rangle_\beta - \sum_{i=2}^{L} \lambda_i(\beta) \langle \hat{H}'^i \rangle_\beta, \quad \hat{H}' = \hat{H} - \langle \hat{H} \rangle_\beta. \tag{A5}$$

In the special case $L = 2$, we obtain ($\hat{Q}' = \hat{Q} - \langle \hat{Q} \rangle_\beta$)

$$\langle \hat{Q} \rangle_E = \langle \hat{Q} \rangle_\beta - \lambda_2(\beta) \langle \hat{H}'^2 \rangle_\beta, \tag{A6}$$

$$\lambda_2(\beta) = \frac{\langle \hat{Q}' \hat{H}'^2 \rangle_\beta \langle \hat{H}'^2 \rangle_\beta - \langle \hat{Q}' \hat{H}' \rangle_\beta \langle \hat{H}'^3 \rangle_\beta}{\langle \hat{H}'^2 \rangle_\beta (\langle \hat{H}'^4 \rangle_\beta - \langle \hat{H}'^2 \rangle_\beta^2) - \langle \hat{H}'^3 \rangle_\beta^2}. \tag{A7}$$

The numerator in Eq. (A7) is exactly equal to that of the saddle point expression (21), but the denominators are different. Expressions (A6) and (21) would coincide if one assumes

$$-\frac{\partial^3 \ln Z}{\partial \beta^3} = \langle \hat{H}'^3 \rangle = 0,$$

$$\frac{\partial^4 \ln Z}{\partial \beta^4} = \langle \hat{H}'^4 \rangle - 3 \langle \hat{H}'^2 \rangle^2 = 0,$$

in the denominator of Eq. (A7), which is in agreement with the Gaussian approximation of the saddle point method. Since these quantities are normally very small in the statistical regime (i.e., for not too low temperatures), Eq. (A6) will be practically coincident with Eq. (21). The present method is essentially an extension of the Lipkin-Nogami method for approximate particle number projection [18] to the case of finite temperature and energy projection. Using an expansion of the form

$$\langle \hat{Q} \rangle_{EN} = \sum_{i,j} \lambda_{ij} (E - E_0)^i (N - N_0)^j, \tag{A8}$$

one can straightforwardly extend this procedure to obtain the microcanonical average for fixed N in the grand canonical ensemble. The saddle point approximation is, however, simpler to apply in the general case and yields both the level density and the microcanonical average.

[1] J.L. Egido and P. Ring, J. Phys. G **19**, 1 (1993).
[2] L.G. Moretto, Phys. Lett. **40B**, 1 (1972).
[3] A.L. Goodman, Nucl. Phys. **A352**, 30 (1981).
[4] A.L. Goodman, Phys. Rev. C **29**, 1887 (1984); **37**, 2162 (1988).
[5] J.L. Egido, P. Ring, S. Iwasaki, and H.J. Mang, Phys. Lett. **154B**, 1 (1985).
[6] R.L. Stratonovich, Dokl. Akad. Nauk. SSSR **115**, 1097 (1957) [Sov. Phys. Dokl. **2**, 458 (1958)].
[7] C.W. Johnson, S.E. Koonin, G.H. Lang, and W.E. Ormand, Phys. Rev. Lett. **69**, 3157 (1992).
[8] G.H. Lang, C.W. Johnson, S.E. Koonin, and W.E. Ormand, Phys. Rev. C **48**, 1518 (1993).
[9] B. Mühlschlegel, D.J. Scalapino, and R. Denton Phys. Rev. B **6**, 1767 (1972).
[10] Y. Alhassid and J. Zingman, Phys. Rev. C **30** 684 (1984).
[11] P. Arve, G.F. Bertsch, B. Lauritzen, and G. Puddu, Ann. Phys. (N.Y.) **183**, 309 (1988).
[12] N. Cerf, Phys. Rev. C **50**, 836 (1994); **49** 852 (1994).
[13] T. Dø̈ssing, *et al.*, Phys. Rev. Lett. **75**, 1276 (1995).
[14] R. Rossignoli, N. Canosa, and P. Ring, Nucl. Phys. **A591**, 15 (1995).
[15] A. Bohr and B. Mottelson, *Nuclear Structure* (Benjamin, Reading, MA, 1969), Vol. I.
[16] R. Rossignoli, Phys. Rev. C **51**, 1772 (1995).
[17] R. Rossignoli and J.L. Egido, Phys. Lett. B **355**, 15 (1995).
[18] H.J. Lipkin, Ann. Phys. **31**, 528 (1960); Y. Nogami, Phys. Rev. **134**, B313 (1964); Y. Nogami and I.J. Zucker, Nucl. Phys. **60**, 203 (1964).
[19] B. Lauritzen, P. Arve, and G.F. Bertsch, Phys. Rev. Lett. **61**, 2835 (1988).
[20] B. Lauritzen and G. Bertsch, Phys. Rev. C **39**, 2412 (1989).
[21] Y. Alhassid and B. Bush, Nucl. Phys. **A549**, 43 (1992).
[22] Y. Alhassid and B. Bush, Nucl. Phys. **A565** 399 (1993).
[23] R. Rossignoli, P. Ring, and N. Dang, Phys. Lett. B **297**, 1061 (1992).
[24] C. Essebag and J.L. Egido, Nucl. Phys. **A552**, 205 (1993).
[25] R. Rossignoli and P. Ring, Ann. Phys. (N.Y.) **235**, 350 (1994).
[26] R. Rossignoli and P. Ring, Phys. Lett. B **337**, 1 (1994).
[27] P. Ring and P. Schuck, *The Nuclear Many-Body Problem* (Springer, New York, 1980).
[28] G. Puddu, P.F. Bortignon, and R.A. Broglia, Phys. Rev. C **42**, 1830 (1990).
[29] G. Puddu, P.F. Bortignon, and R.A. Broglia, Ann. Phys. (N.Y.) **206**, 409 (1991).
[30] M. Baranger and K. Kumar, Nucl. Phys. **A110**, 490 (1968); K. Kumar and M. Baranger, *ibid.* **A110**, 529 (1968).
[31] N. Canosa, H. Miller, A. Plastino, and R. Rossignoli, Physica A **220**, 611 (1995).